

# The Formal Combination of Three Singlet Biradicaloid Entities to a Singlet Hexaradicaloid Metalloid $\text{Ge}_{14}[\text{Si}(\text{SiMe}_3)_3]_5[\text{Li}(\text{THF})_2]_3$ Cluster

Christian Schenk,<sup>†</sup> Andreas Kracke,<sup>†</sup> Karin Fink,<sup>§</sup> Adam Kubas,<sup>§</sup> Wim Klopper,<sup>§,†</sup> Marco Neumaier,<sup>†</sup> Hansgeorg Schnöckel,<sup>†</sup> and Andreas Schnepf<sup>\*,||</sup>

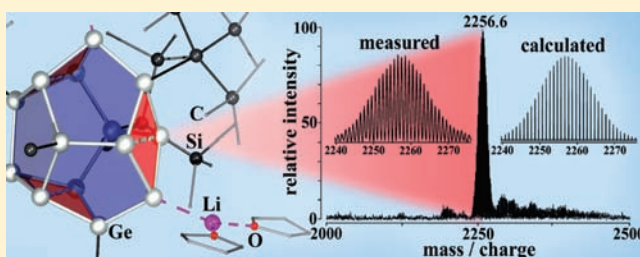
<sup>†</sup>Institut für Anorganische Chemie and <sup>†</sup>Institut für Physikalische Chemie, Karlsruher Institut für Technologie, KIT-Campus Süd, Postfach 6980, D-76049 Karlsruhe, Germany

<sup>§</sup>Institut für Nanotechnologie, Karlsruher Institut für Technologie, KIT-Campus Nord, Postfach 3640, D-76021 Karlsruhe, Germany

<sup>||</sup>Institut für Anorganische Chemie, Universität Duisburg-Essen, Universitätsstrasse 5-7, Raum S07 S03 C49, D-45117 Essen, Germany

**S** Supporting Information

**ABSTRACT:** The reaction of  $\text{GeBr}$  with  $\text{LiSi}(\text{SiMe}_3)_3$  leads to the metalloid cluster compound  $[(\text{THF})_2\text{Li}]_3\text{Ge}_{14}[\text{Si}(\text{SiMe}_3)_3]_5$  (**1**). After the introduction of a first cluster of this type, in which 14 germanium atoms form an empty polyhedron,  $[(\text{THF})_2\text{Li}]_3\text{Ge}_{14}[\text{Ge}(\text{SiMe}_3)_3]_5$  (**2**), we present here further investigations on **1** to obtain preliminary insight into its chemical and bonding properties. The molecular structure of **1** is determined via X-ray crystal structure solution using synchrotron radiation. The electronic structure of the  $\text{Ge}_{14}$  polyhedron is further examined by quantum chemical calculations, which indicate that three singlet biradicaloid entities formally combine to yield the singlet hexaradicaloid character of **1**. Moreover, the initial reactions of **1** after elimination of the  $[\text{Li}(\text{THF})_2]^+$  groups by chelating ligands (e.g., TMEDA or 12-crown-4) are presented. Collision induced dissociation experiments in the gas phase, employing FT-ICR mass spectrometry, lead to the elimination of the singlet biradicaloid  $\text{Ge}_5\text{H}_2[\text{Si}(\text{SiMe}_3)_3]_2$  cluster. The unique multiradicaloid bonding character of the metalloid cluster **1** might be used as a model for reactions and properties in the field of surface science and nanotechnology.



## INTRODUCTION

In recent years, we have established a novel fruitful synthetic route to metalloid cluster compounds of germanium. This was achieved by applying the disproportionation reaction of metastable solutions of the  $\text{Ge}(\text{I})$  halides, namely,  $\text{GeBr}^1$  and  $\text{GeCl}^2$ . These metalloid clusters of the general formula  $\text{Ge}_n\text{R}_m$  ( $n > m$ ,  $\text{R}$  = ligand) can be seen as molecular model compounds for the area between molecules and the solid state,<sup>3</sup> providing valuable insight into the processes that occur during formation, as well as into the dissolution of elemental germanium on an atomic scale, an aspect that is of great significance in the field of nanotechnology. Current studies on such systems act as a first “spotlight” onto this regime, demonstrating the presence of a great structural diversity in this region.<sup>4</sup> In line with this, we were recently able to isolate the largest metalloid cluster compound of germanium,  $[(\text{THF})_2\text{Li}]_3\text{Ge}_{14}[\text{Ge}(\text{SiMe}_3)_3]_5$  (**2**) where the 14 germanium atoms in the cluster core build up to an empty polyhedron, representing a novel structural motif in germanium chemistry. However, the crystal structure solution of **2** proved to be very difficult to obtain, due to a complete disorder of **2** inside the crystal. Only a few crystals of **2** were obtained, providing a first glimpse toward the understanding of this novel cluster compound. These preliminary results were published recently.<sup>5</sup> To address the low yield, we attempted to synthesize similar

compounds by varying just the ligands. Such compounds may potentially show no disorder in the crystal lattice, and may perhaps also show an increase in the yield, paving the way for further investigations on this largest metalloid cluster compound of germanium. As such, bonding properties as well as the chemical behavior of a metalloid  $\text{Ge}_{14}$  cluster should be of fundamental importance for the region between molecules and the solid state. The results presented here provide a deeper understanding of the relevance of the singlet biradicaloid bonding character in molecules, which may be essential for understanding the chemical and physical properties of surfaces or nanostructured materials of group 14.

## RESULTS AND DISCUSSION

**Synthesis.** The synthesis of a metalloid cluster compound similar to **2** is achieved by carrying out the disproportionation reaction of a subhalide. This synthesis is quite difficult to accomplish due to the many reaction steps involved, starting from the binary compound (e.g.,  $\text{GeBr}$ ), all the way to the formation of the metalloid cluster.<sup>6</sup> Nevertheless, **1** could be

Received: August 20, 2010

Published: February 8, 2011

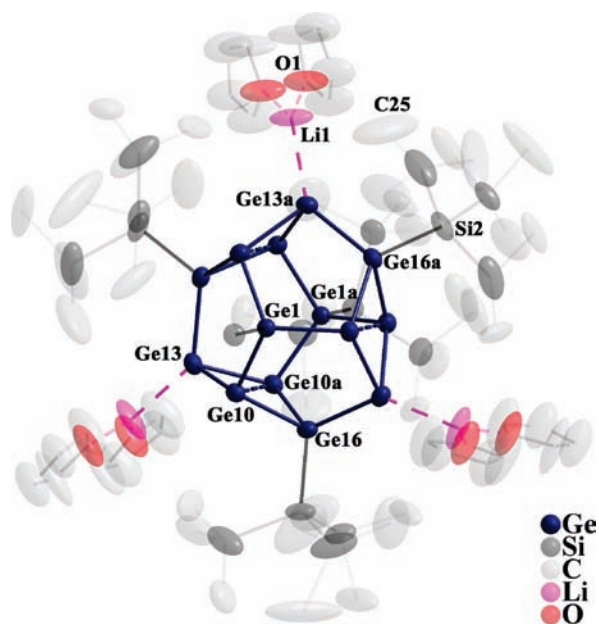


**Figure 1.** Molecular structure of  $\text{Ge}_{14}[\text{Si}(\text{SiMe}_3)_3]_5[\text{Li}(\text{THF})_2]_3$  (**1**) (without hydrogen atoms); vibrational ellipsoids with 50% probability. Selected distances (pm) and angles (deg): Ge1–Ge10, 245.12(9); Ge1–Ge1a, 413.8; Ge13–Ge16a, 658.6; Ge10–Ge13, 249.25(16); Ge10–Ge16, 247.9(2); Ge13a–Ge16a, 256.1(3); Ge10–Ge10a, 283.67(17); Ge1–Si1, 241.7(2); Ge16–Si2, 242.6(4); Ge13–Ge10–Ge16, 108.92(5); Ge10–Ge16–Ge10a, 69.81(9); Ge1–Ge10–Ge13, 109.40(5).

isolated after heating the reaction mixture of GeBr with  $\text{LiSi}(\text{SiMe}_3)_3$  to 80 °C; i.e., we applied similar reaction conditions as for the synthesis of **2**. The nearly black colored reaction solution obtained is heated to 80 °C for 16 h. After changing the solvent to hexane, orange crystals of the well-known metalloid cluster compound  $\text{Ge}_9[\text{Si}(\text{SiMe}_3)_3]_3^-$  (**3**)<sup>7</sup> were isolated in ca. 15% yield.<sup>8</sup>

After the separation of **3**, the hexane solution was still nearly black. We varied the solvent to  $\text{Et}_2\text{O}$  and from this solution obtained another product in the form of dark red, rod-like crystals. X-ray crystal structure analysis of these crystals<sup>9</sup> reveals that the metalloid compound  $\text{Ge}_{14}[\text{Si}(\text{SiMe}_3)_3]_5[\text{Li}(\text{THF})_2]_3$  (**1**) had been formed. The molecular structure is shown in Figure 1. As **1** is obtained in substantial amounts, a more thorough investigation into the chemical behavior of this largest metalloid cluster compound of germanium became possible.

**Structure.** The arrangement of the 14 germanium atoms in the cluster core of **1** is comparable to that of **2**; i.e., a discus-like empty polyhedron of 14 germanium atoms is formed. The  $\text{Ge}_{14}$  polyhedron is composed of six five-membered and three four-membered rings, where the four-membered rings are distorted in a butterfly arrangement, leading to diagonal Ge–Ge distances of 283.7 pm (Ge10–Ge10a). The Ge–Ge distances and Ge–Ge–Ge angles inside **1** and **2** are quite similar, with differences of less than 1%.<sup>10</sup> This structural feature shows that the hollow arrangement of the 14 germanium atoms is quite robust against changes in the ligand shell, also suggesting that bonding within the cluster core is energetically favorable. The hollow arrangement of the 14 germanium atoms in **1** and **2** further shows that the formation of empty polyhedra, i.e., without a stabilizing central atom, is possible even for the heavier congeners of carbon. This also suggests that fullerene-like compounds may be accessible to

germanium, possibly via the mild route of the disproportionation reaction of a Ge(I) halide.

As expected, the main difference between **1** and **2** lies in the bond distance to the ligand; that is, the average Ge–Si distance (242 pm) of **1** is substantially shorter than the average Ge–Ge distance to the ligand in **2** (251 pm). Moreover, the Ge– $\text{SiMe}_3$  distance in **2** (238 pm) is substantially longer than the Si– $\text{SiMe}_3$  distance in **1** (233 pm); i.e., the more compact  $\text{Si}(\text{SiMe}_3)_3$  ligand is bound to the  $\text{Ge}_{14}$  core much more tightly compared to that of the larger  $\text{Ge}(\text{SiMe}_3)_3$  ligand. Despite these differences, there exists a complete shielding of the 14 germanium atoms in the cluster core together with the three  $\text{Li}(\text{THF})_2$  units (Figure S1 in the Supporting Information).

**Classification of the Structure.** The aforementioned geometric arrangement of the 14 germanium atoms in **1** and **2** is unique in the field of molecular compounds. In spite of similarities with a recently described  $\text{Sn}_{14}$  polyhedron found in the Zintl phase  $\text{Na}_{29}\text{Zn}_{24}\text{Sn}_{32}$ ,<sup>11</sup> the differences between the  $\text{Ge}_{14}$  and  $\text{Sn}_{14}$  polyhedra are significant: (a) The  $\text{Sn}_{14}$  polyhedron exhibits planar four-membered rings, leading to a more spherical arrangement of the 14 tin atoms. (b) The  $\text{Sn}_{14}$  polyhedron is not empty; i.e., a sodium cation is present in the center. (c) The  $\text{Sn}_{14}$  polyhedron is a cut-out of the solid state structure. However, the similarities in arrangement of group 14 atoms in a molecular as well as in a solid state compound supports the assumption that such an  $\text{M}_{14}$  polyhedron is a stable structural motif in group 14 chemistry.<sup>12</sup>

Structural similarities of the  $\text{Ge}_{14}$  polyhedron in **1** with the recently reported solid state structure of germanium,  $\text{Ge}(cF136)$ ,<sup>13</sup> are also observed. In  $\text{Ge}(cF136)$ , the germanium atoms are arranged in a clathrate(I) form, exhibiting a substructural motif of a  $\text{Ge}_{20}$  pentagon dodecahedron and a  $\text{Ge}_{28}$  hexacaidecahedron.<sup>14</sup> In both polyhedra, the structural motifs of three directly bound five-membered rings are present, i.e., a similar central structural motif as observed for **1** (Figure S4 in the Supporting Information).

Consequently, with respect to structural similarity, **1** may be seen as an intermediate on the way to the solid state structure of  $\text{Ge}(cF136)$  or to fullerene-like molecular  $\text{Ge}_n$  compounds. Furthermore, because the arrangement of the 10 germanium atoms in the two metalloid cluster compounds  $\{\text{Ge}_{10}(\text{Si}t\text{Bu}_3)_6\text{I}\}^{+15}$  and  $\{\text{Ge}_{10}\text{Si}[\text{Si}(\text{SiMe}_3)_3]_4(\text{SiMe}_3)_2\text{Me}\}^{-2}$  can be described as a structural approach to the solid state structure of  $\alpha$ -germanium, a great variety of structural motifs is realized within this bordering region between molecules and the solid state. The question of which route the larger metalloid cluster compounds with more germanium atoms take should be addressed by forthcoming investigations in the field of metalloid germanium clusters. Nevertheless, the singular arrangement of the 14 germanium atoms in **1** hints at a unique bonding inside the  $\text{Ge}_{14}$  core of the cluster (vide infra).

**Bonding Properties.** *Structural Aspects.* The ligand bound (Ge1, Ge16) and the lithium coordinated (Ge13) germanium atoms exhibit nearly tetrahedral coordination. Furthermore, the Ge–Ge bond distances (245–256 pm) are within the range of a normal Ge–Ge single bond of 245 pm, as found for example in  $\alpha$ -germanium.<sup>16</sup> Hence, one can say that a classical bonding is present here.

With regard to the three pairs of ligand- and lithium-free germanium atoms (Ge10, Ge10a) within the four-membered  $\text{Ge}_4$  units (highlighted in Figure 2), the situation is different for the following reasons. First, the four substituents are not tetrahedrally bound to these atoms.<sup>17</sup> Second, only three Ge–Ge

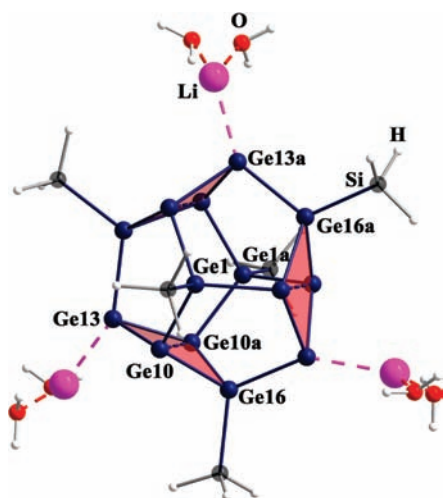


**Figure 2.** Optimized molecular structure of the model compound  $\text{Ge}_{14}(\text{SiH}_3)_5\text{Li}_3(\text{H}_2\text{O})_6$  (**1a**). The three butterfly shaped four-membered rings are emphasized via a polyhedral representation.

distances (245–249 pm) are within the range of a normal Ge–Ge single bond, where the fourth “bond” (Ge10–Ge10a) is significantly elongated (284 pm). The arrangement of the germanium atoms Ge10 and Ge10a actually resembles more of that found for the bridgehead atoms in the  $\text{E}_5\text{R}_6$  propellanes.<sup>18</sup> As a result of these observations, the question of whether the bonding in **1** within the  $\text{Ge}_4$  units is comparable to the aforementioned bonding in propellanes or related compounds arises.<sup>19</sup> High-level quantum chemical calculations are utilized to answer this question.

**Electronic Aspects.** The structure of **1** was optimized with the TURBOMOLE<sup>20</sup> program package at the DFT (density functional theory) level. The gradient corrected BP86 functional with the resolution of the identity (RI) approximation and a def2-SV(P) basis set were employed.<sup>21</sup> The calculated structure belongs to the point group  $C_3$ .<sup>22</sup> In the DFT calculations, a closed shell singlet state was observed. In order to evaluate whether such a closed shell configuration is appropriate in describing the electronic structure of the undercoordinated Ge atoms (Ge10, Ge10a), the CASSCF<sup>23</sup> (complete active space self-consistent field) method was applied. CASSCF is an *ab initio* multireference method in which different electronic configurations can be considered at the same time. To reduce the computational effort, the model compound  $\text{Ge}_{14}(\text{SiH}_3)_5[\text{Li}(\text{H}_2\text{O})_2]_3$  (**1a**), shown in Figure 2, was used in the CASSCF calculations. The structure of **1a** is obtained from the optimized structure of **1**, substituting all  $\text{SiMe}_3$  groups with hydrogen atoms and the THF molecules with  $\text{H}_2\text{O}$ , reoptimizing only the positions of the hydrogen atoms.

The crucial step in a CASSCF calculation is the choice of the “active space”, which is composed of a set of orbitals that are allowed to be partly occupied in the wave function. A systematic way of obtaining the active space is to use the natural orbitals of a ground state MP2 (second-order Møller–Plesset perturbation theory) calculation. At first, we considered all four orbitals with occupation numbers of 1.8–1.9, as well as the seven orbitals with occupations between 0.05 and 0.1 electrons, for inclusion in the active space of the CASSCF calculation. However, after a few optimization steps, it became obvious that only six orbitals were necessary to include in the active space. The other orbitals were

either doubly occupied or empty.<sup>24</sup> The final CASSCF calculations were performed in a [6,6] active space with a def2-TZVP basis set.<sup>25</sup>

Figure 3 shows the six orbitals ( $2a_1$ ,  $2e$ ), together with their orbital energies  $\epsilon$  and occupation numbers  $n$ . These orbitals are linear combinations of those six  $\text{sp}^3$  hybrid orbitals of the six Ge10 atoms, that are not involved in the three classical single bonds. The three strongly occupied orbitals are the symmetry adapted linear combinations of bonding orbitals, while the three weakly occupied orbitals are the corresponding antibonding orbitals. The occupation of the three bonding orbitals is significantly smaller than 2, while the antibonding orbitals show an increase in occupation number. This observation clearly indicates a weakening of the Ge10–Ge10a bonds, in accord with a radicaloid character. As suggested earlier by the geometric structure, the bonding is indeed comparable to the weak bonding between the bridgehead atoms in the  $\text{E}_5\text{R}_6$  propellanes.<sup>18e</sup> This strongly suggests that the three Ge10–Ge10a bonds possess a biradicaloid character.

A quantitative analysis of the bond strength has been obtained from comparison with two model compounds (details of these calculations and figures of the model compounds, Figures S2 and S3, can be found in the Supporting Information). We estimate that the bond strength of the Ge10–Ge10a bond is reduced by 60% in comparison to a typical Ge–Ge single bond. The origin of the biradicaloid character and the reduction in bond strength is the unfavorable orientation of the orbitals which participate in this bond. The orbitals point away from each other due to the arrangement of the other three bonds of the Ge10 centers. If a typical Ge–Ge single bond is stretched to the same length, the binding energy is reduced by only 10–15% and the bonding orbitals remain doubly occupied.

In order to analyze the electronic structure of these bonds in detail, we calculated the relative energy of the three lowest triplet states for **1a** using a state average CASSCF calculation, employing the six partly filled orbitals obtained from the singlet state in this active space (Figure 3). The lowest triplet state is found to be doubly degenerate and 2.11 eV higher in energy than the singlet ground state. The next triplet state is 88.9 meV higher in energy, indicating that a coupling of the three Ge10–Ge10a bonds with biradicaloid character is present in **1**. Thus, from an orbital point of view,  $[(\text{THF})_2\text{Li}]_3\text{Ge}_{14}[\text{Si}(\text{SiMe}_3)_3]_5$  (**1**) can be described as a singlet hexaradicaloid species, which is an extension of the biradicaloid character onto a larger cluster compound.

**Insight from *ab initio* Calculations.** As metalloid clusters are model compounds for the area between molecules and the solid state, the observed multiradicaloid character may also be of importance for nanoparticles and surfaces where unsaturated germanium atoms can be found too. Thus, the emergence of a multiradicaloid character may be the reason for the differences in physical and chemical properties between nanoparticles and the bulk phase; e.g., a strong size-dependent photoluminescence (PL) of germanium nanoparticles is observed even though elemental germanium exhibits no comparable PL.<sup>26</sup> Additionally, the reactivity of a reconstructed  $\text{Ge}(100)\text{-}2 \times 1$  surface with unsaturated organic compounds such as 1,5-cyclooctadiene is normally traced back to the presence of possible “multiple” Ge–Ge bonds.<sup>27</sup> However, a radicaloid character would also lead to a higher reactivity.<sup>28</sup>

These results clearly show a unique bonding for **1**. Due to the multiradicaloid character of **1**, the six Ge10 atoms may be considered as highly reactive centers for attacking reagents, and initial results in this respect are presented below.

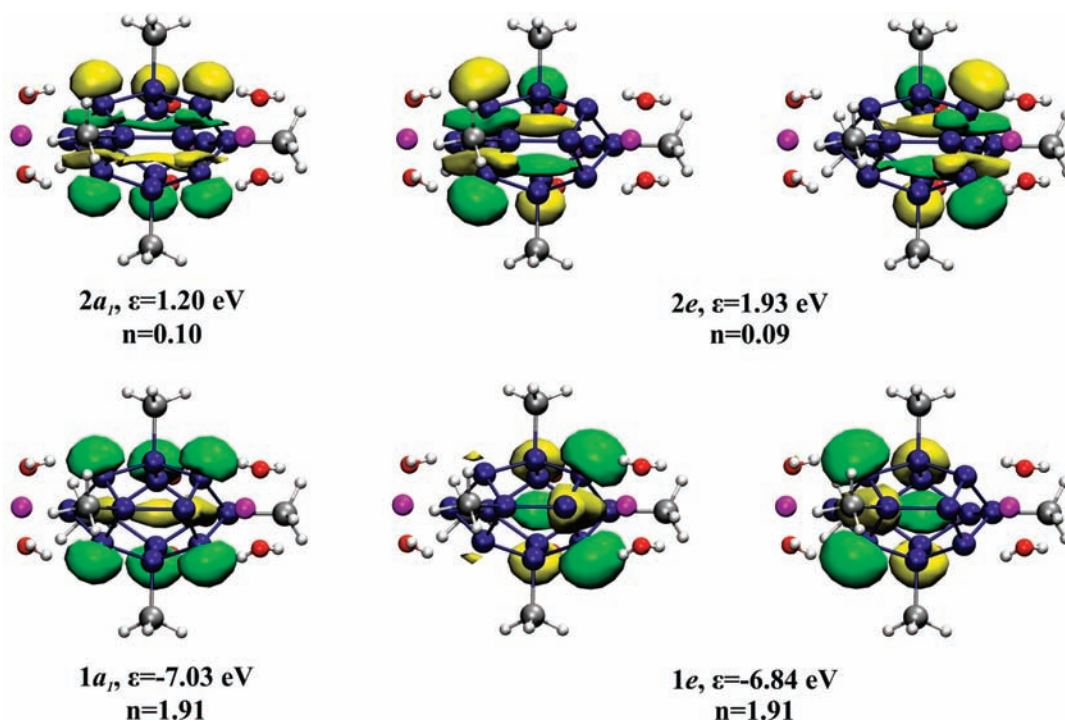
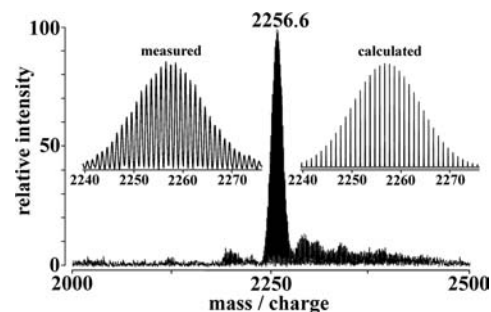


**Figure 3.** Active orbitals of the CASSCF calculations for the singlet ground state of **1a**, with occupation numbers,  $n$ , and energies,  $\epsilon$ , of the respective orbitals. The numbering of orbital numbers  $1a_1$ ,  $1e$ ,  $2a_1$ , and  $2e$  takes into account only the orbitals of the active space.

**Reactivity of [(THF)<sub>2</sub>Li]<sub>3</sub>Ge<sub>14</sub>[Si(SiMe<sub>3</sub>)<sub>3</sub>]<sub>5</sub> (**1**).** *Solution.* As mentioned previously, the germanium core of [(THF)<sub>2</sub>Li]<sub>3</sub>-Ge<sub>14</sub>[Si(SiMe<sub>3</sub>)<sub>3</sub>]<sub>5</sub> (**1**) is completely shielded by five Si(SiMe<sub>3</sub>)<sub>3</sub> and three Li(THF)<sub>2</sub> groups. Furthermore, **1** in solution stays intact; i.e., it can be recrystallized in THF without ion separation; no signals are observed in a mass spectrum of a pure THF solution. The mass spectrometer applied uses a home-built *electrospray ionization source* (ESI)<sup>29</sup> coupled to a commercial FT-ICR-MS (Ionspec, Ultima). With this setup, different metalloid cluster ions have been successfully detected, using THF solutions of dissolved crystals.<sup>8a,8b</sup> Although no ions were detected from a THF solution of **1**, ion signals of the Ge<sub>14</sub> compound **1** were obtained by adding complexing reagents like crown-ethers, such as 12-crown-4 or TMEDA, to the THF solution of **1**, leading to the mass spectrum shown in Figure 4.

Nevertheless, neither the highly charged compound {Ge<sub>14</sub>-[Si(SiMe<sub>3</sub>)<sub>3</sub>]<sub>5</sub>}<sup>3-</sup> (**1b**) ( $m/z = 751.5$ ) nor a lithium coordinated Ge<sub>14</sub> compound like {Ge<sub>14</sub>[Si(SiMe<sub>3</sub>)<sub>3</sub>]<sub>5</sub>Li<sub>2</sub>(THF)<sub>4</sub>}<sup>-</sup> (**1c**) ( $m/z = 2556.8$ ) is observed in high intensity. The dominating signal in the mass spectra can be assigned to the metalloid cluster {Ge<sub>14</sub>[Si(SiMe<sub>3</sub>)<sub>3</sub>]<sub>5</sub>H<sub>2</sub>}<sup>-</sup> (**4**) ( $m/z = 2256.6$ ), whose measured and calculated isotopic patterns are also shown enlarged in Figure 4.<sup>30</sup> Hence, the addition of a complexing reagent leads to ion separation, where the resulting cluster anion is highly reactive, leading to the protonated species **4** (Scheme 1).

A DFT geometry optimization of **4** yields a structure wherein both H atoms are bound to those germanium atoms which were previously bound to the Li(THF)<sub>2</sub> group (Ge<sub>13</sub>), leading to a Ge<sub>14</sub> core that is comparable to that in **1** (Figure 5). This result once again emphasizes the robustness of the Ge<sub>14</sub> polyhedron core. The THF solutions of **1** are very reactive after addition of TMEDA or 12-crown-4; that is, the formerly black solutions decompose overnight even at -28 °C, leading to colorless solutions with a gray precipitate. The increased reactivity can be

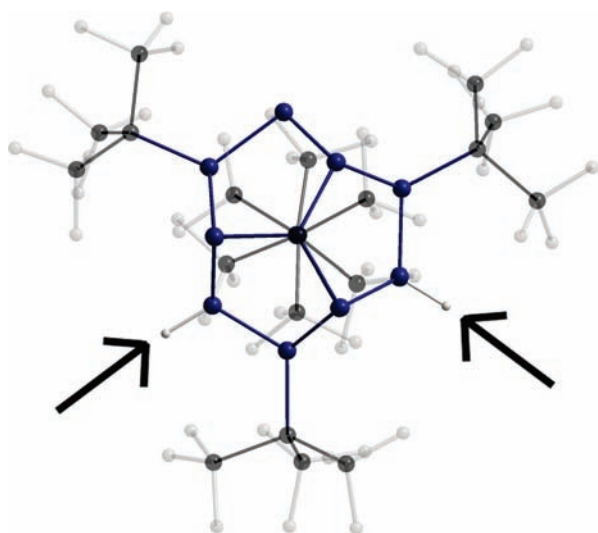
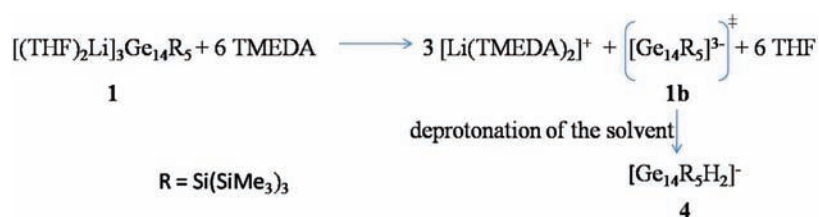
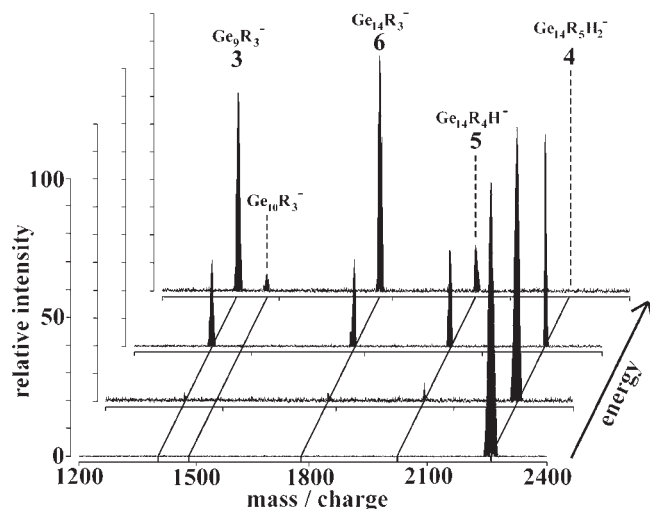


**Figure 4.** FT-ICR mass spectrum of a solution of **1** in THF/toluene/12-crown-4 after electrospray ionization. The inset shows the comparison of the enlarged measured and calculated mass spectra of {Ge<sub>14</sub>-[Si(SiMe<sub>3</sub>)<sub>3</sub>]<sub>5</sub>H<sub>2</sub>}<sup>-</sup> (**4**).

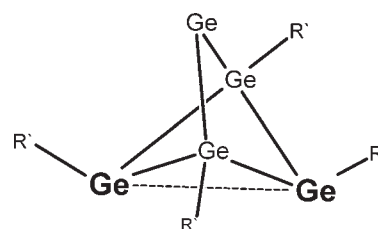
traced back to the removal of the Li(THF)<sub>2</sub> groups, leading to deshielded ligand-free germanium atoms in **1b** (Ge<sub>10</sub>, Ge<sub>10a</sub>, Ge<sub>13</sub>). Apparently, the highly charged cluster {Ge<sub>14</sub>[Si(SiMe<sub>3</sub>)<sub>3</sub>]<sub>5</sub>}<sup>3-</sup> (**1b**) can deprotonate the solvent, initially leading to compounds such as **4**, which in turn decompose to a gray precipitate of unknown composition.

*Gas Phase.* To get a first insight into the decomposition reaction, the cluster anion {Ge<sub>14</sub>[Si(SiMe<sub>3</sub>)<sub>3</sub>]<sub>5</sub>H<sub>2</sub>}<sup>-</sup> (**4**) was isolated in the ICR cell of the FT-ICR-MS. Afterward, the fragmentation of **4** was observed in the gas phase after excitation via SORI-CAD (*sustained off-resonance irradiation collisional activated dissociation*)<sup>31</sup> experiments, leading to different elimination products (Figure 6). These dissociation experiments show that the metalloid cluster {Ge<sub>14</sub>[Si(SiMe<sub>3</sub>)<sub>3</sub>]<sub>5</sub>H<sub>2</sub>}<sup>-</sup> (**4**) fragments after activation, leading to three different product ions with  $m/z = 2008.4$ , 1760.3 and 1396.7. These fragment ions can be assigned to {Ge<sub>14</sub>[Si(SiMe<sub>3</sub>)<sub>3</sub>]<sub>4</sub>H}<sup>-</sup> (**5**) ( $m/z = 2008.4$ ), {Ge<sub>14</sub>[Si(SiMe<sub>3</sub>)<sub>3</sub>]<sub>3</sub>}<sup>-</sup> (**6**) ( $m/z = 1760.3$ ), and the already known metalloid cluster {Ge<sub>9</sub>[Si(SiMe<sub>3</sub>)<sub>3</sub>]<sub>3</sub>}<sup>-</sup> (**3**)

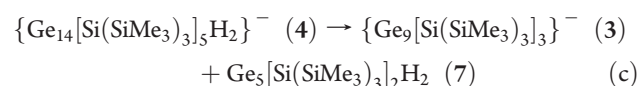
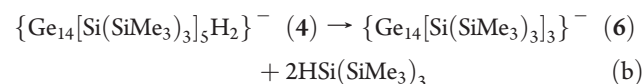
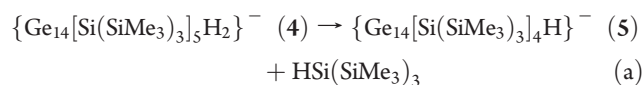
Scheme 1. Reaction Sequence for the Formation of 4 after Addition of a Complexing Reagent Such as TMEDA to a THF Solution of 1

Figure 5. Calculated structure of the metalloid germanium cluster  $\{\text{Ge}_{14}[\text{Si}(\text{SiMe}_3)_3]_5\text{H}_2\}^-$  (4) (without carbon-bound hydrogen atoms). The arrows point to the two additional H atoms.Figure 6. FT-ICR mass spectra detected at different activation energies. Lowest energy: Signal of the isolated ion 4 ( $m/z = 2256.6$ ). Higher energies: Parent ion 4 and its fragment ions ( $m/z = 2008.4$ ;  $1760.3$ ;  $1396.7$ ). The intensity of the detected fragment ions increases at higher SORI-CAD energies ( $\text{R} = \text{Si}(\text{SiMe}_3)_3$ ).

( $m/z = 1396.7$ ).<sup>7</sup> The smaller signal at  $1468.6$  is most likely due to the presence of  $\{\text{Ge}_{10}[\text{Si}(\text{SiMe}_3)_3]_3\}^-$  as a minor fragmentation product of 4. All three main fragment ions have similar intensities

Figure 7. Molecular structure of  $\text{Ge}_5\text{R}_4$  (8) ( $\text{R}' = \text{CH}(\text{SiMe}_3)_2$  or 2,6-Mes<sub>2</sub>-C<sub>6</sub>H<sub>3</sub>; Mes = 2,4,6-Me<sub>3</sub>-C<sub>6</sub>H<sub>2</sub>). The two germanium atoms with coordination number 3 are emphasized in bold representation.

in the dissociation experiment; i.e., all intensities increase as the internal energy increases, showing that parallel routes (eqs a–c) with energetically similar activation barriers are present.<sup>32</sup>



The most unusual result of the collision induced dissociation experiments is the elimination of the neutral  $\text{Ge}_5\text{H}_2$ - $[\text{Si}(\text{SiMe}_3)_3]_2$  cluster (7), leading to the stable metalloid  $\text{Ge}_9[\text{Si}(\text{SiMe}_3)_3]_3^-$  cluster (3). The eliminated neutral cluster might possess the structure of the recently described metalloid cluster  $\text{Ge}_5\text{R}'_4$  (8) ( $\text{R}' = \text{CH}(\text{SiMe}_3)_2$  or 2,6-Mes<sub>2</sub>-C<sub>6</sub>H<sub>3</sub>; Mes = 2,4,6-Me<sub>3</sub>-C<sub>6</sub>H<sub>2</sub>),<sup>33</sup> where a  $\text{Ge}_4\text{R}'_4$  rectangle, distorted in a butterfly arrangement, is capped by a ligand-free germanium atom (Figure 7). As the bonding between the two germanium atoms with coordination number 3 in 8 also exhibits a biradicaloid character, a direct connection between a singlet biradicaloid and a singlet hexaradicaloid system is present via this dissociation channel in the gas phase.

## CONCLUSION AND OUTLOOK

The reaction of  $\text{GeBr}$  with  $\text{LiSi}(\text{SiMe}_3)_3$  leads to a second isostructural example of a metalloid  $\text{Ge}_{14}$  cluster compound, which is the largest structurally characterized metalloid cluster for germanium to date. Such a polyhedral arrangement is robust against changes in the ligand shell, owing to the fact that only minor distortions of the  $\text{Ge}_{14}$  polyhedron in the cluster core of 1 and 2 are

observed. Because the yield of isolated crystals of  $[(\text{THF})_2\text{Li}]_3\text{Ge}_{14}[\text{Si}(\text{SiMe}_3)_3]_5$  (**1**) was quite high, more extensive investigations were made possible. Such investigations led to an improved understanding of the bonding within this metalloid  $\text{Ge}_{14}$  cluster, revealing its relevance in nanotechnology and surface science.

CASSCF quantum chemical calculations provide important clues into the unusual bonding situation within the  $\text{Ge}_{14}$  polyhedron, showing that the long bond in each of these  $\text{Ge}_4$  subunits of the  $\text{Ge}_{14}$  polyhedron exhibits a singlet biradicaloid character. Because three of these subunits are present in the  $\text{Ge}_{14}$  polyhedron,  $[(\text{THF})_2\text{Li}]_3\text{Ge}_{14}[\text{Si}(\text{SiMe}_3)_3]_5$  (**1**) can be described as a singlet hexaradicaloid species. Consequently, as metalloid clusters are ideal model compounds for the area between molecules and the solid state, such multiradicaloid character may very well be of importance to nanoparticles and surfaces where subvalent atoms play a significant role. The expected high reactivity of the ligand-free germanium atoms in **1** can be shown by first subsequent reactions. These reactions can be carried out after the elimination of the  $[\text{Li}(\text{THF})_2]^+$  groups by chelating ligands such as TMEDA or 12-crown-4, eventually leading to a complete decomposition. Gas phase mass spectrometer measurements of **1** via collision induced fragmentation indicate that the trianion **1b** is highly reactive and deprotonates the solvent, leading to the protonated species  $\{\text{Ge}_{14}[\text{Si}(\text{SiMe}_3)_3]_5\text{H}_2\}^-$  (**4**). Dissociation experiments of **4** in the gas phase via FT-ICR mass spectrometry provide a first glimpse into the reaction course of the decomposition. At this stage, neutral  $\text{H}-\text{Si}(\text{SiMe}_3)_3$  molecules are eliminated, giving a less shielded  $\text{Ge}_{14}$  compound. In solution, this  $\text{Ge}_{14}$  compound could be an intermediate on the way to the gray, possibly germanium-rich precipitate, we observed during our experiments. If this reactivity can be reduced, the anionic intermediates can perhaps be used as building blocks for further build-up reactions. Additionally, the elimination of a singlet biradicaloid  $\text{Ge}_5\text{H}_2[\text{Si}(\text{SiMe}_3)_3]_2$  cluster, similar to that presented recently, further validates the importance of such a multiradicaloid bonding character in compounds belonging to the border region between molecules and the solid state.

## EXPERIMENTAL SECTION

**Synthesis.** Liquid germanium was treated with HBr at 1550 °C, and the resulting gaseous GeBr molecules were subsequently condensed with a solvent mixture of toluene/ $\text{N}^m\text{Pr}_3$  (10:1) at -196 °C. The solid condensate (20 mmol of GeBr) was then warmed to -78 °C, giving an emulsion of a dark red oil in a pale yellow solution. This emulsion was treated at -78 °C with a toluene solution of  $\text{Li}\{\text{Si}(\text{SiMe}_3)_3\} \cdot 3\text{THF}$  (10.3 g, 20 mmol). The reaction mixture was then slowly warmed up to room temperature, producing a nearly black solution. Removal of the solvent in vacuum yielded a black oil. Extraction of this oil with heptane gives a black heptane solution, which was stored at 80 °C for 16 h. A white precipitate was filtered, and storage of the heptane extract at 6 °C gave orange crystals, which are recrystallized from THF, leading to  $[\text{Ge}_9\{\text{Si}(\text{SiMe}_3)_3\}_3]\text{Li}(\text{THF})_4$  (540 mg, 0.33 mmol, 14.8%). The solvent of the remaining heptane extract was changed to  $\text{Et}_2\text{O}$ , and the resulting black  $\text{Et}_2\text{O}$  solution gave dark red, almost black crystals of  $[\text{Ge}_{14}\{\text{Si}(\text{SiMe}_3)_3\}_5][\text{Li}(\text{THF})_2]_3 \cdot [\text{Si}(\text{SiMe}_3)_4] \cdot \text{Et}_2\text{O}$  (143 mg, 0.05 mmol, 3.5%) at -28 °C.

**Crystal Structure Analysis.** Crystal structure data for  $[\text{Ge}_{14}\{\text{Si}(\text{SiMe}_3)_3\}_5][\text{Li}(\text{THF})_2]_3 \cdot [\text{Si}(\text{SiMe}_3)_4] \cdot \text{Et}_2\text{O}$ :  $\text{Ge}_{14}\text{Si}_{25}\text{O}_7\text{C}_{85}\text{Li}_3\text{H}_{229}$ ,  $M_r = 3098.4 \text{ g mol}^{-1}$ , crystal dimensions  $0.4 \times 0.2 \times 0.2 \text{ mm}^3$ , hexagonal, space group  $P6_3/m$ ,  $a = 20.1775(6) \text{ \AA}$ ,  $c = 21.9148(7) \text{ \AA}$ ,  $V = 7726.9(4) \text{ \AA}^3$ ,  $Z = 2$ ,  $\rho_{\text{calcd}} = 1.312 \text{ g cm}^{-3}$ ,  $\mu_{\text{Mo}} = 2.909 \text{ mm}^{-1}$ ,  $2\theta_{\text{max}} = 52.16^\circ$ , 21115 measured, 3389 independent reflections ( $R_{\text{int}} = 0.0709$ ),

absorption correction: numerical (min/max transmission 0.4403/0.5992),  $R_1 = 0.0471$ ,  $wR_2 = 0.0975$ , STOE IPDS II diffractometer (ANKA synchrotron radiation ( $\lambda = 0.8 \text{ \AA}$ ), 150 K. The structure was solved by direct methods and refined against  $F^2$  for all observed reflections. Programs used: SHELXS and SHELXL.<sup>34</sup> CCDC-785494 contains the supplementary crystallographic data for this paper. These data can be obtained free of charge from the Cambridge Crystallographic Data Centre via [www.ccdc.cam.ac.uk/data\\_request/cif](http://www.ccdc.cam.ac.uk/data_request/cif).

**Mass Spectrometry.** Mass spectrometric experiments were performed on an IonSpec Ultima FT-ICR-MS (Fourier transform ion cyclotron resonance mass spectrometer), equipped with a 7 T superconducting magnet, coupled to a home-built electrospray ionization source (ESI).<sup>29</sup> The cluster  $\{\text{Ge}_{14}[\text{Si}(\text{SiMe}_3)_3]_5\text{H}_2\}^-$  (**4**) was brought into the gas phase by electrospraying a solution of the  $\text{Ge}_{14}$  compound **1** in THF after addition of complexing reagents like crown-ethers, e.g., 12-crown-4 or TMEDA. The end-plate of the electrospray source was typically held at a potential of +3.2 kV, and a potential of +3.3 kV was applied to the metal coated quartz capillary. Prior to ion transfer into the ICR cell through several differential pumping stages, the ions were stored in a hexapole ion trap in order to accumulate ions and to adopt the continuously working ESI source to the pulsed ICR technique. After ion transfer, **4** was isolated by a SWIFT (stored waveform inverse Fourier transform) excitation.<sup>35</sup> In order to dissociate the  $\{\text{Ge}_{14}[\text{Si}(\text{SiMe}_3)_3]_5\text{H}_2\}^-$  ions by the SORI (sustained off-resonance irradiation collisional activated dissociation) technique, a short (4 ms) gas pulse of argon was admitted into the ICR cell, raising the pressure to  $\sim 1 \times 10^{-6}$  mbar. Then, the anions of **4** were excited in the presence of argon by applying an off-resonant dipolar radio frequency (rf) pulse at a frequency of  $\sim 1.5\%$  lower than the reduced cyclotron frequency of the ions for the duration of 1000 ms. The collision energy was varied by changing the voltage of the rf excitation pulse. Ion detection took place after a pumping delay of ca. 12 s at  $\sim 5 \times 10^{-10}$  mbar.

## ASSOCIATED CONTENT

**S Supporting Information.** Comparison of **1** and **2**; space filling model of  $\text{Ge}_{14}[\text{Si}(\text{SiMe}_3)_3]_5[\text{Li}(\text{THF})_2]_3$  (**1**); calculations concerning the bond strength between  $\text{Ge}_{10}-\text{Ge}_{10a}$  (diagonal in the  $\text{Ge}_4$  unit); calculated structure of **4** and structural clarification of the relation of **1** and  $\text{Ge}(cF136)$ . Discussion of the dissociation routes of **4** in the gas phase. This material is available free of charge via the Internet at <http://pubs.acs.org>.

## AUTHOR INFORMATION

### Corresponding Author

\*Phone: Int. Code +49 (201) 183 - 3684. Fax: Int. Code +49 (201) 183 - 3830. E-mail: [andreas.schnepf@uni-due.de](mailto:andreas.schnepf@uni-due.de).

## ACKNOWLEDGMENT

We thank the Deutsche Forschungsgemeinschaft (DFG) for support through the Center for Functional Nanostructures (CFN, subprojects C1.3 and C3.3). Furthermore, we thank the KIT for beamtime at the synchrotron ANKA and Dr. G. Buth for help with the measurements. We also thank Dr. Ericka C. Barnes for helpful discussions.

## REFERENCES

- (1) Köppe, R.; Schnepf, A. *Z. Anorg. Allg. Chem.* **2002**, *628*, 2914–2918.
- (2) Schnepf, A. *Chem. Commun.* **2007**, 192–194.
- (3) Schnepf, A. *Coord. Chem. Rev.* **2006**, *250*, 2758–2770.
- (4) Schnepf, A. *New J. Chem.* **2010**, *34*, 2079–2092.
- (5) Schenk, C.; Schnepf, A. *Chem. Commun.* **2008**, 4643–4645.

(6) As Ge–Ge distances are with 245 pm comparable to Ge–Si distances of 238 pm, a similar  $\text{Ge}_{14}$  compound might be obtained applying the  $\text{Si}(\text{SiMe}_3)_3$  ligand, where the central germanium atom of the  $\text{Ge}(\text{SiMe}_3)_3$  ligand is changed by a silicon atom.

(7) Schnepf, A. *Angew. Chem.* **2003**, *115*, 2728–2729; *Angew. Chem., Int. Ed.* **2003**, *42*, 2624–2625.

(8) Heating the reaction mixture of  $\text{GeBr}$  with  $\text{LiSi}(\text{SiMe}_3)_3$  to 80 °C leads to a greater than 100% increase in yield of the  $\text{Ge}_9$  compound **3** (the yield was only 7% without heating). Since **3** is the starting material for further build-up reactions on the way to novel materials (e.g., anionic  $\{\text{Ge}_{18}\text{M}[\text{Si}(\text{SiMe}_3)_3]_6\}^-$ ,  $\text{M} = \text{Cu}, \text{Ag}, \text{Au}$ , or neutral  $\text{Ge}_{18}\text{M}[\text{Si}(\text{SiMe}_3)_3]_6$ ,  $\text{M} = \text{Zn}, \text{Cd}, \text{Hg}$ ), this result is a significant improvement for this chemistry based on **3**: (a) Schenk, C.; Henke, F.; Santigo, G.; Krossing, I.; Schnepf, A. *Dalton Trans.* **2008**, 4436–4441; (b) Schenk, C.; Schnepf, A. *Angew. Chem.* **2007**, *119*, 5408–5410; *Angew. Chem., Int. Ed.* **2007**, *46*, 5314–5316. (c) Henke, F.; Schenk, C.; Schnepf, A. *Dalton Trans.* **2009**, *42*, 9141–9145. (d) Schnepf, A. *Eur. J. Inorg. Chem.* **2008**, 1007–1018.

(9) The measurement was performed at the synchrotron light source ANKA at the Research Center of Karlsruhe as the same disorder is present in **1** as it was the case in **2**. Thus, **1** cocrystallizes with  $\text{Si}(\text{SiMe}_3)_4$  in the hexagonal crystal system in the space group  $P6_3/m$ , whereby a disorder of the molecule is present which is described by a statistic model (58:42% occupancy). However, refinement of the data applying a split model only leads to a very bad  $R_1$  value of 24.62% ( $wR_2 = 54.48\%$ ). The situation is more complicated, owing to the presence of merohedral twinning of the crystal. Applying the twin matrix (0 1 0, 1 0 0, 0 0 –1) leads to a drop in the  $R_1$  value to 4.28% ( $wR_2 = 9.53\%$ ), where the BASF value was refined to 0.49986. As the disorder is still present, the change of the ligand thus leads to a more complicated system as the crystals are additionally merohedrally twinned, with the twinning element of a 2-fold axis. However, as we found the twin law, the crystal structure could be satisfactorily solved.

(10) A comparison of the Ge–Ge distances and Ge–Ge–Ge angles is listed in the Supporting Information (Table S1).

(11) Kim, S.-J.; Hoffman, S. D.; Fässler, T. F. *Angew. Chem.* **2007**, *119*, 3205–3209; *Angew. Chem., Int. Ed.* **2007**, *46*, 3144–3148.

(12) A comparable  $\text{Ge}_{14}$  arrangement was recently calculated for the minimum structure of the tetra-anion  $\text{Ge}_{14}^{4-}$ : King, R. B.; Silaghi-Dumitrescu, I.; Uta, M. M. *Eur. J. Inorg. Chem.* **2008**, 3996–4003.

(13) Guloy, A. M.; Ramlau, R.; Tang, Z.; Schnelle, W.; Baitinger, M.; Grin, Y. *Nature* **2006**, *443*, 320–323.

(14) Fässler, T. F. *Angew. Chem.* **2007**, *119*, 2624–2628; *Angew. Chem., Int. Ed.* **2007**, *46*, 2572–2575.

(15) Sekiguchi, A.; Ishida, Y.; Kabe, Y.; Ichinohe, M. *J. Am. Chem. Soc.* **2002**, *124*, 8776–8777.

(16) *Holleman-Wiberg Lehrbuch der Anorganischen Chemie*, 102nd ed.; Wiberg, N.; Wiberg, E., Holleman, A., Eds.; de Gruyter & Co.: Berlin, 2007; pp 1002–1041.

(17) The arrangement might be described as “inverse tetrahedral,” as introduced by Wiberg et al. for the metalloid silicon compound  $\text{Si}_8\text{-}(\text{Si}t\text{Bu}_3)_6$ : Fischer, G.; Huch, V.; Vasisht, M. S. K.; Veith, M.; Wiberg, N. *Angew. Chem.* **2005**, *117*, 8096–8099; *Angew. Chem., Int. Ed.* **2005**, *44*, 7884–7887.

(18) (a) Sita, L. R.; Bickerstaff, R. D. *J. Am. Chem. Soc.* **1989**, *111*, 6454–6456; (b) Drost, C.; Hildenbrand, M.; Lönnecke, P. *Main Group Met. Chem.* **2002**, *25*, 93–98; (c) Richards, A. F.; Power, P. P. *Organometallics* **2004**, *23*, 4009–4011; (d) Nied, D.; Klopper, W.; Breher, F. *Angew. Chem.* **2009**, *121*, 1439–1444; *Angew. Chem., Int. Ed.* **2009**, *48*, 1411–1416. (e) Nied, D.; Köppe, R.; Klopper, W.; Schnöckel, H.; Breher, F. *J. Am. Chem. Soc.* **2010**, *132*, 10264–10265.

(19) Breher, F. *Coord. Chem. Rev.* **2007**, *251*, 1007–1043.

(20) TURBOMOLE V6.0 2009, a development of University of Karlsruhe and Forschungszentrum Karlsruhe GmbH, 1989–2007, TURBOMOLE GmbH, since 2007; available from <http://www.turbomole.com>.

(21) BP86: Becke, A. D. *Phys. Rev. A* **1988**, *38*, 3098–3100. Perdew, J. P. *Phys. Rev. B* **1986**, *33*, 8822–8824. *def2-SV(P)*: Schäfer, A.; Horn, H.; Ahlrichs, R. *J. Chem. Phys.* **1992**, *97*, 2571–2577. *RI*: Eichkorn, K.

Treutler, O.; Öhm, H.; Häser, M.; Ahlrichs, R. *Chem. Phys. Lett.* **1995**, *242*, 652. Eichkorn, K.; Weigend, F.; Treutler, O.; Ahlrichs, R. *Theor. Chem. Acc.* **1997**, *97*, 119. Weigend, F. *Phys. Chem. Chem. Phys.* **2006**, *8*, 1057–1065.

(22) The calculated structures and minimum energies are virtually identical in point group  $C_3$  and  $C_1$ . However, for the CASSCF calculations, the optimized  $C_1$  structure was used, while the classification of the orbitals was performed for point group  $C_3$  (*a* and *e*).

(23) Roos, B. O.; Tylor, P. R.; Siegbahn, P. E. M. *Chem. Phys.* **1980**, *48*, 157–173.

(24) All CASSCF and MP2 calculations have been performed with the program package ORCA: ORCA V2.7.0, an Ab Initio, DFT and Semiempirical electronic structure package developed by Frank Neese, Lehrstuhl für Theoretische Chemie, Institut für Physikalische und Theoretische Chemie, Universität Bonn, Germany; available from <http://www.thch.uni-bonn.de/tc/orca/>.

(25) Schäfer, A.; Huber, C.; Ahlrichs, R. *J. Chem. Phys.* **1994**, *100*, 5829.

(26) Maeda, Y.; Tsukamoto, N.; Yazawa, Y.; Kanemitsu, Y.; Masumoto, Y. *Appl. Phys. Lett.* **1991**, *59*, 3168–3170. Yang, H.; Yang, R.; Wan, X.; Wan, W. *J. Cryst. Growth* **2004**, *261*, 549–556.

(27) Prayongpan, P.; Stripe, D. S.; Greenlief, C. M. *Surf. Sci.* **2008**, *602*, 571–578.

(28) For reconstructed  $\text{Si}(100)\text{-}2 \times 1$  surfaces, the significance of radicals was lately shown for the cooperative bifluorination or bichlorination: Harikumar, K. R.; Leung, L.; McNab, I. R.; Polanyi, J. C.; Lin, H.; Hofer, W. A. *Nat. Chem.* **2009**, *1*, 716–721.

(29) Burgert, R. Dissertation, Universitätsverlag Karlsruhe, 2007.

(30) Above  $m/z = 2270$ , overlapping less intense signals are observed which might be assigned to monoanionic  $\{\text{Ge}_{14}[\text{Si}(\text{SiMe}_3)_3]_5\text{-X}_2\}^-$  clusters exhibiting combinations of  $\text{X} = \text{H}^+$ ,  $[\text{Li}(\text{THF})_2]^+$ , and  $[\text{Li}(12\text{-crown-}4)]^+$  coordinated to  $\{\text{Ge}_{14}[\text{Si}(\text{SiMe}_3)_3]_5\}^{3-}$  (**3b**). However, an exact assignment is not possible due to the small intensity.

(31) Gauthier, J. W.; Trautman, T. R.; Jacobsen, D. B. *Anal. Chim. Acta* **1991**, *246*, 211–225.

(32) The presence of parallel reaction channels was corroborated by a further experiment, where the fragment ion **5** was continuously removed by a dipolar on-resonant excitation during the SORI fragmentation of the parent ion **4**. The same experiment was performed with **6** being removed continuously. During this procedure, the relative intensity of the respectively lower fragment ions did not change. This shows that all three fragment ions **5**, **6**, and **7** are directly generated from the fragmentation of the parent ion **4** in a parallel reaction mechanism, without being obligatory intermediates for lower mass fragment ions.

(33) Richards, A. F.; Brynda, M.; Olmstead, M. M.; Power, P. P. *Organometallics* **2004**, *23*, 2841–2844.

(34) Sheldrick, G. M. *Acta Cryst.* **2008**, *A64*, 112–122.

(35) Wang, T. C. L.; Ricca, T. L.; Marshall, A. G. *Anal. Chem.* **1986**, *58*, 2935–2938.